

Fast Non-Monte-Carlo Transient Noise Analysis for High-Precision Analog/RF Circuits by Stochastic Orthogonal Polynomials^{*}

Fang Gong
University of California, Los Angeles
Electrical Engineering Department
Los Angeles, CA 90095, US
gongfang@ucla.edu

Hao Yu
Nanyang Technological University
School of Electrical and Electronic Engineering,
Singapore
haoyu@ntu.edu.sg

Lei He
University of California, Los Angeles
Electrical Engineering Department
Los Angeles, CA 90095, US
lhe@ee.ucla.edu

ABSTRACT

Stochastic device noise has become a significant challenge for high-precision analog/RF circuits, and it is particularly difficult to correctly include both white noise and flicker noise in the traditional transient verification with an efficient numerical solution. In this paper, a Non-Monte-Carlo transient noise analysis is developed. Both white noise and flicker noise are considered in Itô integral based stochastic differential algebraic equation (SDAE), which is solved by one-time calculation of variance using stochastic orthogonal polynomials (SoPs). Our work is the first in literature to provide the SoP-based SDAE solution with application for transient noise analysis. Experiments on a number of different analog circuits demonstrate that the proposed method is up to 488X faster than Monte Carlo method with similar accuracy, and achieves on average 6.8X speedup over the existing non-Monte-Carlo approaches.

Categories and Subject Descriptors: B.7.[Hardware]: - Integrated Circuits-Design Aids

General Terms: Algorithms, Performance

Keywords: Noise analysis, Circuit simulation

1. INTRODUCTION

Device noise is one of fundamental limits for circuit performance. Noise-related issues are particularly critical for high-precision circuits implemented at nanometer-scale with low voltages or high frequencies. For example, random device noise has a significant impact on CMOS PLL phase noise and jitter[1]. The noise-sensitive analog/RF circuits such as ADCs and PLLs are the core components for bio-sensory and wireless communication systems.

The device random noise is primarily composed of white noise (thermal and shot) and flicker noise. Thermal noise is broadband white noise that intensifies as temperature increases. In contrast,

^{*}The project is partially supported by UC Discovery Grant and Singapore MOE ACRF TIER-1 grant under No.M5204016.

Permission to make digital or hard copies of all or part of this work for personal or classroom use is granted without fee provided that copies are not made or distributed for profit or commercial advantage and that copies bear this notice and the full citation on the first page. To copy otherwise, to republish, to post on servers or to redistribute to lists, requires prior specific permission and/or a fee.

DAC'11, Jun 05-10 2011, San Diego, CA, USA.

Copyright 2011 ACM 978-1-4503-0636-2/11/06 ...\$10.00.

flicker noise is due to defects in semiconductor. The frequency at which the flicker-noise spectral density intersects the flat white-noise spectral density is called *1/f corner frequency*. Both thermal and flicker noise can be modeled inside the device model of one transistor. The primary challenge is to verify the transient noise behavior at circuit and system level with multiple transistors. The traditional SPICE-like verification assumes either small-signal ac noise or periodic steady-state noise analysis in a linear fashion, which cannot satisfy the need to accurately verify the nonlinear transient noise analysis.

Mainly due to the stochastic characteristic of device noise, the design for high-precision analog/RF components is usually time-consuming. The efficient numerical analysis of the transistor-level transient noise is required to facilitate the high-precision analog/RF designs in the nanometer region. A number of previous arts have been proposed to address the aforementioned challenge when verifying the transient device noise. Based on the Itô integral formulation, the transient noise can be estimated by solving the stochastic differential algebraic equations (SDAE) either under Euler-Maruyama or Milstein method [2, 3]. One recent work in [4] has applied the stochastic integral scheme for SDAE, in particular stochastic analogues of the backward differentiation formula (BDF) and implicit trapezoidal rule (ITR) as in the traditional SPICE tools. However, this approach still requires the expensive Monte-Carlo iterations with the use of sampling-paths at each time point. Moreover, expensive correlation analysis is required to calculate the noise variance. In addition, it is unknown how to model flicker noise inside this framework.

In [5, 6], a time-domain non-Monte-Carlo noise simulation considering thermal noise has been developed. Device noises are modeled as uncorrelated stochastic current sources. Since the magnitude of the noise in a signal is much smaller when compared to the magnitude of the signal itself, the solution of SDAE can be first piecewise-linearized along the nominal trajectory. The resulting reformulated SDAE is then solved by the perturbation analysis. In order to calculate the noise variance, this approach also needs to perform the correlation analysis with intensive matrix-operations on the covariance matrix of circuit state variables at each time point, though the need of Monte Carlo iterations is avoided. The evaluation using the covariance matrix is expensive for the large-scale transient analysis. More importantly, because the perturbation analysis in [5, 6] is not applied to SDAE under the Itô-integral form, the reformulation of SDAE under perturbation analysis might be inaccurate.

In this paper, we present an efficient and accurate non-Monte-Carlo transient noise analysis to verify the stochastic noise of high-precision analog/RF circuits. First, it can model not only thermal noise but also flicker noise in the time domain. The flicker noise is modeled by synthesized RC networks with white noise current sources, which can be connected to noise-free circuit elements. This leads to one unified Itô-integral formed SDAE. Next, in order to avoid inefficient Monte Carlo iterations and

expensive co-variance matrix analysis [4, 5] when calculating the noise variance, we propose one-time calculation with the use of stochastic orthogonal polynomials (SoPs). To the best of our knowledge, it is the first time to present the SoP solution for Itô integral based SDAE in literature. Experiments show that SoP based method is up to 488X faster than Monte Carlo method with similar accuracy. When compared with previous work, SoPs method can provide on average 6.8X speedup and higher accuracy.

The rest of the paper is organized as follows. We review the background of noise models and SoPs in Section 2. We briefly summarize the previous work in Section 3 and discuss our SoP based method in Section 4 with details. We show experiment results in Section 5 and conclude in Section 6.

2. BACKGROUND

2.1 Noise Models

2.1.1 White Noise Model

Both thermal noise and shot noise can be modeled as one white Gaussian noise current source connected in parallel with an ideal circuit element such as a noise-free resistor or current source.

For instance, the thermal noise current for resistor is

$$i_{th}(t) = \sqrt{\frac{2kT}{R}} \xi(t) \quad (1)$$

where k is Boltzmann's constant, T is the absolute temperature and R is the resistance. $\xi(t)$ is a standard Gaussian white noise process, which is stationary with a constant power spectral density (PSD) in frequency domain.

Similarly, there exists white noise in the channel of one MOS transistor associated with transconductance g_m by

$$i_{th}(t) = \sqrt{4kT\theta \cdot g_m} \cdot \xi(t). \quad (2)$$

where θ depends on channel length and operating region [7] with varied value from 1/2 to 2/3.

2.1.2 Flicker Noise Model

Flicker noise is dominant in MOS transistors, which can be modeled by another noise current in parallel. The PSD of flicker noise in MOS transistor can be generally written as

$$S_i(f) = \frac{i_f^2}{\Delta f} = \frac{K_F}{C_{ox}WL} \times g_m^2 \times \frac{1}{f} \quad (3)$$

where W is channel width, L is channel length and C_{ox} is gate oxide capacitance per unit area. Note that K_F here is flicker noise coefficient, a constant depending on the process technology. g_m is transconductance of MOS transistor and f is the frequency.

From equation (3), flicker noise has a time-varying PSD as a function of frequency. Since it is a non-stationary noise process, flicker noise cannot be included in the transient noise analysis in [4]. With the use of synthesized RC circuit [5, 6], one can generate the summation of Lorentzian spectra in (4) to approximate the 1/f noise PSD by

$$S(f) = \frac{2kT}{\pi C_m} \sum_{m=1}^M \frac{\varphi_m}{\varphi_m^2 + f^2} \propto \frac{1}{f}. \quad (4)$$

As shown in Fig(1), φ_m is the pole-frequency and each Lorentzian spectra, which is represented by a *white noise* current source together with an pair of resistor R_m and capacitor C_m in parallel.

In general, each flicker noise source can be represented by an ideal voltage-controlled current source $i(t)$ and $i(t) = g(t) \cdot v(t)$. $v(t)$ is the output voltage of one R_m - C_m group circuit in Fig(1) and $g(t)$ is a time-varying transconductance. When capacitor C_m is fixed with constant value C , $g(t)$ can be written as

$$g(t) = g_m \sqrt{\frac{K_F}{C_{ox}WL} \cdot \frac{\pi C}{2kT}} \quad (5)$$

Here, g_m is the transconductance of MOS transistor. This important result shows that one can always model flicker noise by the synthesized RC networks and white noise current sources.

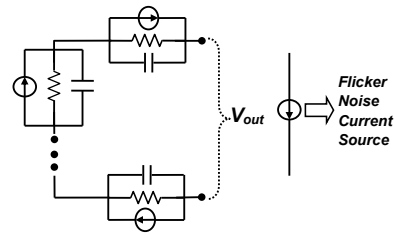


Figure 1: Flicker current noise source synthesis

2.2 Stochastic Orthogonal Polynomial

One recent advance in stochastic analysis is to apply stochastic orthogonal polynomial [8] or polynomial chaos [9] to efficiently estimate stochastic variance. Based on the *Askey scheme*, any stochastic random variable can be represented by stochastic orthogonal polynomials (SoPs), and the random variable with different type of probability distribution is related to different type of SoP.

For example, for white noise current source with random variable $\xi(\psi)$, where $\psi \sim N(0, 1)$, $\xi(\psi)$ can be spanned by Hermite polynomials $\Phi(\psi) = [1, \psi, \psi^2 - 1, \dots]^T$ as

$$\xi(\psi) = \alpha_0 \Phi_0 + \alpha_1 \Phi_1 + \alpha_2 \Phi_2 + \dots = \sum_{i=0}^n \alpha_i \Phi_i. \quad (6)$$

Note that SoPs satisfy the following orthogonal property:

$$\langle \Phi_i(\psi), \Phi_j(\psi) \rangle = \langle \Phi_i^2(\psi) \rangle \cdot \delta_{ij} \quad (7)$$

where δ_{ij} is the Kronecker delta and $\langle *, * \rangle$ denotes an inner product operation.

As such, when the SoP representation is available, the mean and variance of $\xi(\psi)$ can be obtained from one-time calculation:

$$\begin{aligned} E(\xi(\psi)) &= \alpha_0 \\ Var(\xi(\psi)) &= \alpha_1^2 + 2\alpha_2^2 \end{aligned} \quad (8)$$

In this paper, we show how to apply the SoP technique as the non-Monte-Carlo solution for the transient device noise analysis.

3. PREVIOUS WORK

One integrated circuit is composed of many devices described by many terminal-branch equations. It can be formally described by differential-algebraic equation (DAE)

$$A \frac{d}{dt} q(x(t), t) + f(x(t), t) = 0 \quad (9)$$

under KCL's law. Here, $x(t)$ is vector of state variables consisting of node voltages and branch currents. $q(x(t), t)$ contains charges and fluxes and $f(x(t), t)$ describes the terminal current-voltage relation. The constant matrix A is incidence matrix determined by circuit topology.

3.1 Itô Integral based SDAE

When device noises become the interest, they are modeled by noise current sources added to the above deterministic DAE (9)

$$\underbrace{A \frac{d}{dt} q(x(t), t) + f(x(t), t)}_{\text{deterministic}} + \underbrace{\sum_{r=1}^m g_r(x(t), t) \xi_r(t)}_{\text{stochastic}} = 0 \quad (10)$$

where $g_r(x(t), t)$ is vector of noise intensities, and $\xi_r(t)$ is vector of noise sources (White noise). (10) is called *stochastic differential-algebraic equation (SDAE)*. Although (10) only differs from (9) by the stochastic noise sources, it requires a completely different numerical analysis. The primary difficulty to solve SDAE is that the required derivative of $x(t)$ is unavailable since $x(t)$ is nowhere differentiable due to the influence of stochastic noise sources.

Note that (10) can be interpreted as a stochastic Itô integral equation by integrating over one small time-interval $[t_0, t]$:

$$Aq(x(s))|_{t_0}^t + \int_{t_0}^t f(x(s), s)ds + \sum_{r=1}^m \int_{t_0}^t g_r(x(t), t)dW_r(t) = 0. \quad (11)$$

The second integral part is called Itô Integral and the equation (11) is called *Itô Integral based SDAE* [10, 4]. $W_r(t)$ denotes the Brownian motion or the Wiener Process, obtained by integrating the white noise: $W_r(t) = \int_0^t \xi_r(s)ds = \int_0^t dW_r(s)$. One Wiener process is characterized by the initial value $W(0) = 0$ and the independent non-overlapping increment $\Delta W(t_n) = W(t_n) - W(t_{n-1}) \sim N(0, h_n)$, where $h_n = t_n - t_{n-1}$ is the time-step.

Under the the form of Itô Integral based SDAE, the work in [10] proved the existence and uniqueness of the solution. The work in [4] further derived several stochastic integration methods for SDAE. For example, one accurate stochastic two-step backward differentiation formula (BDF2)-Maruyama method can be applied for the discretization of (11)

$$A \frac{q(x_n) - \frac{4}{3}q(x_{n-1}) + \frac{1}{3}q(x_{n-2}))}{h} + \frac{2}{3}f(x_n) + \sum_{r=1}^m g_r(x_{n-1}) \frac{\Delta W_n^r}{h} - \frac{1}{3} \sum_{r=1}^m g_r(x_{n-2}) \frac{\Delta W_{n-1}^r}{h} = 0. \quad (12)$$

At each time step, (12) can be solved by Newton method with a number of Monte Carlo based sampling-paths due to the Wiener process ΔW_r . The noise variance is calculated afterwards at each time-step with Monte Carlo iterations. This forms the foundation for the transient noise analysis in [4, 10]. The limitation of this approach is the inefficiency due to the Monte Carlo iterations, where the complexity increases with the number of noise sources and the scale of circuits.

3.2 Perturbation based SDAE

Considering that the magnitude of noise (1nV or -100dB) is much smaller than the magnitude of signal, it is appropriate to solve SDAE for transient noise application by the perturbation analysis [5, 6]. One can first obtain the nominal transient trajectory or solution $x^{(0)}(t)$ for (9). The SDAE in (10) is then piecewise-linearized

$$A \left[\frac{d}{d}q(x^{(0)}(t)) + \frac{\partial q(x(t))}{\partial x} \Big|_{x=x^{(0)}} \cdot (\dot{x}(t) - \dot{x}^{(0)}(t)) \right] + \left[f(x^{(0)}(t), t) + \frac{\partial f(x(t))}{\partial x} \Big|_{x=x^{(0)}} \cdot (x(t) - x^{(0)}(t)) \right] + \sum_{r=1}^m g_r(x^{(0)}(t), t)\xi_r(t) = 0. \quad (13)$$

For the simplicity of illustration, one can define following notations based on the nominal solution of (9):

$$C^{(0)}(t) = \frac{\partial q(x(t))}{\partial x} \Big|_{x=x^{(0)}}, \quad G^{(0)}(t) = \frac{\partial f(x(t))}{\partial x} \Big|_{x=x^{(0)}} \\ \Delta x = x(t) - x^{(0)}(t), \quad \Delta \dot{x} = \dot{x}(t) - \dot{x}^{(0)}(t) \\ F = \sum_{r=1}^m g_r(x(t), t). \quad (14)$$

As such, the linearized SDAE is simplified as

$$A \cdot C^{(0)}(t) \cdot \Delta \dot{x} + G^{(0)}(t) \cdot \Delta x + F \cdot \xi(t) = 0. \quad (15)$$

Instead of transforming (15) into Itô Integral based SDAE as (11), [5] theoretically decoupled the SDAE into an inherent stochastic differential equation (SDE) and an algebraic constraint. We notice that such a decoupling is appropriate to simplify the numerical analysis but may also compromise the accuracy [4], which is demonstrated by our experiments as well.

For the decoupling, [5] reordered variables Δx so that zero columns of $C^{(0)}(t)$ are grouped at the right-hand side of the matrix as $C^{(0)}(t)$ may contain zero columns. As such, (15) becomes:

$$\begin{bmatrix} C_{11}(t) & 0 \\ 0 & 0 \end{bmatrix} \begin{bmatrix} \Delta \dot{x}_1 \\ \Delta \dot{x}_2 \end{bmatrix} + \begin{bmatrix} G_{11}(t) & G_{12}(t) \\ G_{21}(t) & G_{22}(t) \end{bmatrix} \begin{bmatrix} \Delta x_1 \\ \Delta x_2 \end{bmatrix} + \begin{bmatrix} F_1(t) \\ F_2(t) \end{bmatrix} \xi = 0 \quad (16)$$

where $C_{11}(t)$ consists of non-zero columns of $A \cdot C^{(0)}(t)$. This results in an inherent stochastic differential equation (SDE) with one additional algebraic constraint by

$$\begin{aligned} G_{11}(t)\Delta x_1 + G_{12}(t)\Delta x_2 + C_{11}(t)\Delta \dot{x}_1 + F_1(t)\xi &= 0 \\ G_{21}(t)\Delta x_1 + G_{22}(t)\Delta x_2 + F_2(t)\xi &= 0 \\ \Delta x &= \begin{bmatrix} \Delta x_1 & \Delta x_2 \end{bmatrix}^T. \end{aligned} \quad (17)$$

The first equation in (17) owns the standard SDE form.

Rather than performing Monte Carlo iterations to calculate the noise variance, [5, 6] applied non-Monte-Carlo approach to calculate the noise variance from the covariance matrix. Based on the *Itô theorem*[11], the covariance matrix $K_1(t)$ for the SDE in (17) can be expressed in the differential Lyapunov matrix equation by

$$\begin{aligned} \dot{K}_1(t) &= - \left(G_{11}(t) + G_{12}(t) \cdot \left(-(G_{22}(t))^{-1} G_{21}(t) \right) \right) K_1(t) \\ &+ K_1(t) \left[- \left(G_{11}(t) + G_{12}(t) \cdot \left(-(G_{22}(t))^{-1} G_{21}(t) \right) \right) \right]^T \\ &+ \left[- \left(F_1(t) + G_{12}(t) \cdot \left(-(G_{22}(t))^{-1} F_2(t) \right) \right) \right] \\ &\cdot \left[- \left(F_1(t) + G_{12}(t) \cdot \left(-(G_{22}(t))^{-1} F_2(t) \right) \right) \right]^T. \end{aligned} \quad (18)$$

As such, the covariance matrix $K_1(t_n)$ can be obtained from the above correlation analysis at time step t_n , and variances of circuit variables at t_n can be further extracted from the diagonal elements of $K_1(t_n)$. Though this method avoids massive samplings and iterations from Monte Carlo, there is a number of time-consuming operations to solve the inherent SDE numerically and to perform the expensive operations on the Lyapunov matrix.

4. SOP BASED NMC TRANSIENT NOISE ANALYSIS

As discussed in Section 3, the primary challenge of the transient noise analysis is lack of the efficient yet accurate analysis. Moreover, a complete transient noise solution needs to include flicker noise. Applying stochastic orthogonal polynomials (SoPs) to obtain the variance by one-time calculation, we develop the non-Monte-Carlo transient noise analysis in this section.

4.1 Itô Integral based SDAE with Flicker Noise

We denote the synthesized RC network for flicker noise as *synthesized circuit*. There are two equivalent approaches to count the contribution of flicker noise:

- **Static Method:** Flicker noise is computed beforehand by performing transient noise analysis on the synthesized circuit using (12). Afterward, the flicker noise is injected into the original circuit for the total transient noise analysis.
- **Dynamic Method:** The original circuit is first augmented with the corresponding synthesized circuits. Then, transient noise analysis is performed on the augmented circuit using (12).

The dynamic method requires to create extra nodes for the synthesized circuit and thus increases the complexity. In this paper, we take the static method as an example for the illustration, but the proposed technique can be applied to the case of dynamic method in a similar fashion.

Let $i_f^k(t)$ be the value of k -th white noise current source for the flicker noise. Since flicker noises can be modeled as additive noise current sources, (10) becomes

$$A \underbrace{\frac{d}{dt}q(x(t)) + f(x(t), t)}_{\text{noise free}} + \underbrace{\sum_{k=1}^n T_k \cdot i_f^k(t)}_{\text{flicker noise}} + \underbrace{\sum_{r=1}^m g_r(x(t), t)\xi_r(t)}_{\text{thermal noise}} = 0 \quad (19)$$

where T_k is topology matrix determining how to connect flicker noise current sources in the circuit.

Similarly, in order to obtain the Itô integral based SDAE with flicker noise, (19) can be integrated over the time-interval by

$$Aq(x(s))\Big|_{t_0}^t + \int_{t_0}^t f(x(s), s)ds + \sum_k \int_{t_0}^t T_k \cdot i_f^k(t) \cdot ds + \sum_{r=1}^m \int_{t_0}^t g_r(X(t), t)dW_r(t) = 0. \quad (20)$$

The corresponding BDF₂-Maruyama method with only increments of Wiener process at n -th discretized time instant is then derived by

$$A \frac{q(x_n) - \frac{4}{3}q(x_{n-1}) + \frac{1}{3}q(x_{n-2})}{h} + \frac{2}{3}f(x_n) + \frac{1}{2} \sum_k T_k \cdot i_f^k(t_n) + \sum_{r=1}^m g_r(x_{n-1}) \frac{\Delta W_n^r}{h} - \frac{1}{3} \sum_{r=1}^m g_r(x_{n-2}) \frac{\Delta W_{n-1}^r}{h} = 0. \quad (21)$$

Table 1: SoP Expansions for Random Variables.

Random Variables	SoP Expansion	
known variables	$i_f^k(t_n)$ ΔW_n^r	$g(t_n) \cdot (\gamma_0^k(t_n)\Phi_0 + \gamma_1^k(t_n)\Phi_1 + \dots)$ $\alpha_0^r(t_n)\Phi_0 + \alpha_1^r(t_n)\Phi_1 + \dots$
unknown variables	$q(x_n)$	$q(x_n^{(0)}) + C_n^{(0)} \cdot (\beta_1(t_n)\Phi_1 + \dots)$
	$f(x_n)$	$f(x_n^{(0)}) + G_n^{(0)} \cdot (\beta_1(t_n)\Phi_1 + \dots)$
	x_n	$x_n^{(0)}\Phi_0 + \beta_1(t_n)\Phi_1 + \dots$

4.2 SoP based Galerkin Method of SDAE

The above equation (21) and (12) can be solved with Monte Carlo iterations, which is very inefficient. We develop an efficient Non-Monte-Carlo (NMC) transient noise analysis using stochastic orthogonal polynomials (SoPs), which leads to one-time calculation of the noise variance. In the following, we will discuss how to represent random variables in (21) by SoPs and solve x_n by Galerkin method. Note that random variables in this section include $q(x_n)$, $f(x_n)$, ΔW_n^r , $i_f^k(t)$ and x_n , whose SoP representations are discussed below and summarized in Table 1.

4.2.1 SoP Expansions of $q(x_n)$ and $f(x_n)$

Since the magnitudes of both white noise and flicker noise are much smaller than the one of signal, one can first obtain the nominal transient solution $x_n^{(0)}$ and accordingly $q(x_n^{(0)})$ and $f(x_n^{(0)})$. Along this nominal transient trajectory, x_n , $q(x_n)$ and $f(x_n)$ can be piecewise-linearized by

$$\begin{aligned} x_n &= x_n^{(0)} + \Delta x_n \\ q(x_n) &= q(x_n^{(0)}) + \frac{\partial q}{\partial x} \Big|_{x=x_n^{(0)}} \cdot \Delta x_n \\ f(x_n) &= f(x_n^{(0)}) + \frac{\partial f}{\partial x} \Big|_{x=x_n^{(0)}} \cdot \Delta x_n. \end{aligned} \quad (22)$$

As such, one only needs to solve for the stochastic perturbation $\Delta x_n = x_n - x_n^{(0)}$ instead of x_n . Note that Δx_n has Gaussian distribution with noise mean is $E(\Delta x_n) = 0$ and hence $E(x_n) = x_n^{(0)}$. Moreover, the noise variance is $Var(x_n) = Var(\Delta x_n)$, which leads to the SoP expansions of x_n and Δx_n by

$$\begin{aligned} \Delta x_n &= 0 \cdot \Phi_0 + \beta_1(t_n)\Phi_1 + \dots \\ x_n &= x_n^{(0)} + \Delta x_n = x_n^{(0)}\Phi_0 + \beta_1(t_n)\Phi_1 + \dots \end{aligned} \quad (23)$$

Accordingly, one can obtain the SoP expansions of $q(x_n)$ and $f(x_n)$ by

$$\begin{aligned} q(x_n) &= q(x_n^{(0)}) + C_n^{(0)} \cdot (\beta_1(t_n)\Phi_1 + \dots) \\ f(x_n) &= f(x_n^{(0)}) + G_n^{(0)} \cdot (\beta_1(t_n)\Phi_1 + \dots) \end{aligned} \quad (24)$$

Here, capacitive and conductive Jacobians are used for the simplicity of notation

$$C_n^{(0)} = \frac{\partial q}{\partial x} \Big|_{x=x_n^{(0)}}; G_n^{(0)} = \frac{\partial f}{\partial x} \Big|_{x=x_n^{(0)}}.$$

4.2.2 SoP Expansion of ΔW_n^r and $i_f^k(t_n)$

The increments of Wiener process $\Delta W_n^r \sim N(0, h_n)$ can be represented by SoPs as

$$\Delta W_n^r = \alpha_0^r(t_n)\Phi_0 + \alpha_1^r(t_n)\Phi_1 + \alpha_2^r(t_n)\Phi_2 + \dots \quad (25)$$

With techniques in [9], $\alpha_i^r(t_n)$ can be obtained with one known distribution of ΔW_n^r . Take the first-order expansion as an example, $\alpha_0^r(t_n) = E(\Delta W_n^r) = 0$, and $(\alpha_1^r(t_n))^2 = Var(\Delta W_n^r) = h_n$.

In addition, the SoP expansion of k -th flicker noise current source $i_f^k(t_n)$ becomes

$$i_f^k(t_n) = g(t_n) \cdot v(t_n) = g(t_n) \cdot [\gamma_0^k(t_n)\Phi_0 + \gamma_1^k(t_n)\Phi_1 + \dots]. \quad (26)$$

Here, $g(t)$ is the transconductance defined in (5). $v(t)$ is the output voltage of flicker noise synthesized circuit in Fig.(1), which only contains thermal noises and can be solved with BDF₂-Maruyama method in (12) under the scheme of static method.

4.2.3 Solution of γ_i by SoP based Galerkin Method

Because the static method is considered to calculate the contribution of flicker noise, $\{\gamma_i\}$ needs to be first determined by the SoP based Galerkin method. By expanding $q(x_n)$, $f(x_n)$ and ΔW_n^r via SoPs for the synthesized circuit, one can obtain a new SDAE under BDF₂-Maruyama discretization described in (27) at the top of next page. By applying the inner-product with Φ_i ($i = 0, 1, \dots$) to (27), one can obtain a set of equations corresponding to the order of SoPs for $\gamma_i(t_n)$.

For example, the resulting Φ_1 becomes

$$\begin{aligned} A \frac{C_n^{(0)} \cdot \gamma_1(t_n) - \frac{4}{3}C_{n-1}^{(0)} \cdot \gamma_1(t_{n-1}) + \frac{1}{3}C_{n-2}^{(0)} \cdot \gamma_1(t_{n-2})}{h} \\ + \left(\frac{2}{3}G_n^{(0)} \cdot \gamma_1(t_n) \right) + \frac{2}{3} \sum_{r=1}^m g_r \cdot \frac{\alpha_1(t_n)}{h} = 0. \end{aligned} \quad (28)$$

As a result, $\gamma_i(t_n)$ can be solved from (28).

4.2.4 Solution of x_n by SoP based Galerkin Method

When the contribution from the flicker noise is obtained, one can further obtain the total transient noise by one more SoP based Galerkin method. By applying the inner-product with Φ_i ($i = 0, 1, \dots$) to (21), coefficients β_i of SoP expansion for x_n in (23) can be computed. For instance, the equation corresponding to Φ_1 is

$$\begin{aligned} A \frac{C_n^{(0)} \cdot \beta_1(t_n) - \frac{4}{3}C_{n-1}^{(0)} \cdot \beta_1(t_{n-1}) + \frac{1}{3}C_{n-2}^{(0)} \cdot \beta_1(t_{n-2})}{h} \\ + \left(\frac{2}{3}C_n^{(0)} \cdot \beta_1(t_n) \right) + \frac{1}{2} \sum_k T_k \cdot g_k(t_n) \cdot \gamma_1^k(t_n) \\ + \frac{2}{3} \sum_{r=1}^m g_r \cdot \frac{\alpha_1(t_n)}{h} = 0. \end{aligned} \quad (29)$$

$$\begin{aligned}
& A \cdot \frac{\left(q(x_n^{(0)}) + C_n^{(0)} \cdot \sum_{i=0}^n \gamma_i(t_n) \Phi_i \right)}{h} - A \cdot \frac{4}{3} \cdot \frac{\left(q(x_{n-1}^{(0)}) + C_{n-1}^{(0)} \cdot \sum_{i=0}^n \gamma_i(t_{n-1}) \Phi_i \right)}{h} + A \cdot \frac{1}{3} \cdot \frac{\left(q(x_{n-2}^{(0)}) + C_{n-2}^{(0)} \cdot \sum_{i=0}^n \gamma_i(t_{n-2}) \Phi_i \right)}{h} \\
& + \left(\frac{2}{3} \left(f(x_n^{(0)}) + G_n^{(0)} \cdot \sum_{i=0}^n \gamma_i(t_n) \Phi_i \right) \right) + \frac{2}{3} \sum_{r=1}^m g_r \frac{\sum_{i=0}^n \alpha_i(t_n) \Phi_i}{h} = 0.
\end{aligned} \tag{27}$$

The above equation can be solved for $\beta_1(t_n)$ at n -th time instant and is repeatedly solved for all time instants. As a result, β_i can be calculated as a function of time. Therefore, the noise variance at t_n can be efficiently obtained by $Var(x_n) = \{\beta_1(t_n)\}^2$.

5. EXPERIMENTAL RESULTS

We have implemented the proposed non-Monte-Carlo transient noise analysis in a Matlab based SPICE-like circuit simulator, and all experiments are carried out on Linux servers with 2.4GHz Xeon processor and 4GB memory. We use SoP method for two purposes: SoP expansion of flicker noise in Section 5.1, and SoP expansion for transient noise analysis in Section 5.2. Two analog circuits including a CMOS comparator and a 3-stage ring oscillator are used to compare with Monte Carlo and Perturbation based SDAE analysis [5]. We include both thermal noise and flicker noise sources in our simulation.

5.1 SoP Expansion to Model Flicker Noise

SoP expansion of flicker ($1/f$) noise is validated by standard deviation of $1/f$ noise (σ_{noise}) in the time domain. Using the synthesized circuit in Fig.(1), we perform both 1000 Monte Carlo simulations and SoP method to generate $1/f$ noise σ_{noise} as a function of time. The speedup of SoP method over Monte Carlo simulations is $1030.85(s)/1.01(s) \approx 1020X$. Fig.(2) shows the σ_{noise} from both methods. Initially, there are large differences, but error reduces as time increases. Note that the difference at initial stage is not important since simulation time of flicker noise is always in long time-scale. In fact, the average error of SoP method with respect to Monte Carlo is only 0.32%.

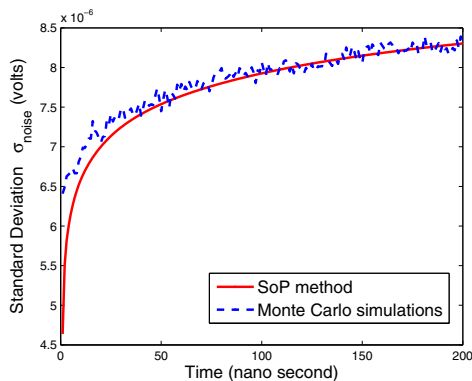


Figure 2: σ_{noise} comparison for the flicker ($1/f$) noise

5.2 SoP Method for Transient Noise Analysis

5.2.1 Accuracy for CMOS Comparator

The first example is one CMOS comparator as shown in Fig.(3) and detailed information about the post layout of this circuit is illustrated in Table (2). We consider both thermal noise and flicker noise to all eight MOSFETs, while only thermal noise is considered for all resistors.

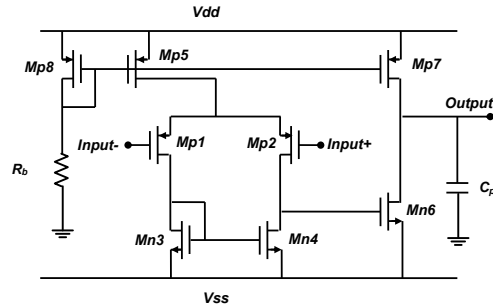


Figure 3: A CMOS comparator implementation with PMOS input drivers

First, we run Monte Carlo simulations to capture the standard deviation (σ_{output}) of impacted output voltage with 0.5% error level in the time domain. It is denoted as one red dash-line with plus-sign in Fig (4). Then, perturbation-based SDAE analysis [5] is conducted for σ_{output} which leads to a black-dash line with cross-sign. In addition, the σ_{output} from SoP method is marked by a blue dash-line with triangle-sign.

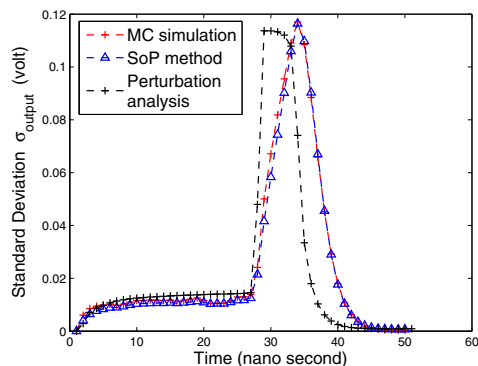


Figure 4: Comparison of σ_{output} for comparator

From the comparison in Fig (4), SoP method fits with Monte Carlo simulations very well in the time domain, while perturbation-based SDAE analysis[5] has low accuracy in the pulse area. This shows that SoP method can provide higher accuracy. The total CPU runtime is in Table (3) and our SoP method is the fastest.

5.2.2 Accuracy for 3-stage CMOS Ring-oscillator

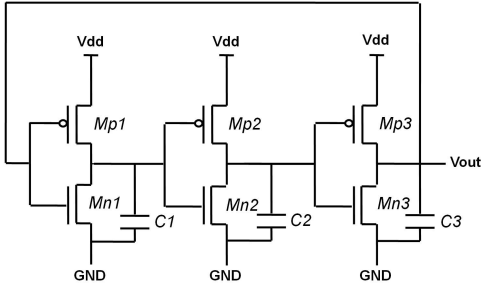
We further consider a 3-stage ring-oscillator as shown in Fig(5) and post-layout details are listed in Table(2). Similarly, we study the standard deviation of output voltage σ_{output} in this example.

We first introduce thermal noises and $1/f$ noises to all MOS-FETs and run Monte Carlo simulations to obtain σ_{output} with 0.5% error level, which is plotted as a red dash-line with plus-sign in Fig.(6). Note that σ_{output} is not constant as a function

Table 2: Circuit Information for Different Examples.

circuit example	#nodes	#devices	#thermal noise	#flicker noise
CMOS Inverter	13	21	10	1
OPAM	46	61	43	8
Comparator	41	54	37	8
Oscillator	37	57	37	6

of time, because $1/f$ noise is one non-stationary random process and its PSD is not a constant in frequency domain. Then, perturbation based SDAE analysis is performed to generate σ_{output} as one black dash-line with cross-sign. Additionally, our proposed SoP method computes σ_{output} denoted by one blue dash-line with triangle-sign, visually identical to Monte Carlo results.

**Figure 5: A 3-stage CMOS ring-oscillator**

As shown in Fig.(6), the perturbation-based SDAE analysis can provide satisfied accuracy during low-to-high and high-to-low transitions, but fails in the peak region. In contrast, our SoP method is able to obtain high accuracy within the entire region. In fact, the accuracy of all methods are compared in Table.(3). Monte Carlo simulation can provide high accuracy (0.5% error), and perturbation based SDAE analysis has error up to 36% loss. SoP method achieves the similar accuracy by 1% error.

Table 3: Accuracy and Total Runtime Comparison for Different Circuit Examples. (Time Unit: second)

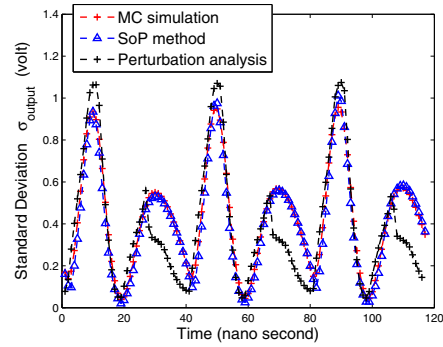
method		Inverter	OPAM	Comparator	Oscillator
		error	0.5%	0.5%	0.5%
MC method	time	91.95	4266.64	2226.71	146851.2
	speedup	1X	1X	1X	1X
	error	5.24%	18.6%	36.4%	33.7%
Pert. ¹ analysis	time	1.84	54.71	12.56	304.3
	speedup	50X	78X	177X	483X
	error	0.43%	0.93%	1.78%	1.62%
SoP method	time	1.87	52.35	12.72	300.91
	speedup	49X	81.5X	175X	488X

¹ Perturbation based SDAE analysis

5.2.3 Runtime Comparison

We further compare the runtime in Table.(3). Monte Carlo method is inefficient, and the perturbation-based SDAE analysis and our SoP method have similar efficiency with up to 488X speedup. Recall that our SoP method can provide higher accuracy. Note that the total runtime for non-Monte-Carlo (NMC) methods in Table.(3) contains both nominal transient simulation time and standard deviation σ_{output} computation time, where the nominal transient analysis dominates the total runtime. We further compare the runtime of σ_{output} computation for both NMC methods in Table(4). As shown in the table, SoP method is around 6.8X faster than the perturbation based SDAE analysis[5], and this speed advantage is expected to be bigger when the scale of studied circuit increases.

6. CONCLUSION

**Figure 6: Comparison of σ_{output} for Oscillator****Table 4: Runtime for σ_{output} computation.**

circuit example	Perturbation Analysis		SoP Method	
	time (s)	speedup	time (s)	speedup
CMOS Inverter	0.06	1X	0.013	4.6X
OPAM	3.07	1X	0.41	7.5X
Comparator	1.36	1X	0.168	8.1X
Oscillator	5.46	1X	0.8	6.8X

In this paper, Itô integral based stochastic differential algebraic equation (SDAE) is deployed to consider both white and flicker noise for high precision analog/RF circuits. One non-Monte-Carlo solution is developed based on the stochastic orthogonal polynomial (SoP) to solve the piecewise-linearized SDAE. The noise variance can be obtained by just one-time calculation at each time-point. Extensive experiments demonstrate that our proposed method is up to 488X faster than Monte Carlo method with a similar accuracy, and achieves on average 6.8X speedup over existing non-Monte-Carlo method.

7. REFERENCES

- [1] A. Mehrotra, "Noise analysis of phase-locked loops," in *Proc. IEEE/ACM ICCAD*, 2000.
- [2] G. N. Milstein, "Numerical integration of stochastic differential equations," 2005.
- [3] P. E. Kloeden and E. Platen, "Numerical solution of stochastic differential equations," 1999.
- [4] G. Denk, W. Romisch, T. Sickenberger, and R. Winkler, "Efficient transient noise analysis in circuit simulation," *Proc. in Applied Math. and Mechanics*, vol. 6, pp. 55–58, 2006.
- [5] A. Demir, E. W. Y. Liu, and A. L. Sangiovanni-Vincentelli, "Time-domain non-Monte Carlo noise simulation for nonlinear dynamic circuits with arbitrary excitations," in *Proc. IEEE/ACM ICCAD*, pp. 598–603, 1994.
- [6] A. Demir, E. W. Y. Liu, and A. L. Sangiovanni-Vincentelli, "Time-domain non-Monte Carlo noise simulation for nonlinear dynamic circuits with arbitrary excitations," *Computer-Aided Design of Integrated Circuits and Systems, IEEE Transactions on*, vol. 15, no. 5, pp. 493–505, 1996.
- [7] Y. Cheng, M. Chan, K. Hui, M. Jeng, Z. Liu, J. Huang, K. Chen, J. Chen, R. Tu, P. K. Ko, and C. Hu, "BSIM3v3 manual," *Univ. California at Berkeley*, 1996.
- [8] S. Vrudhula, J. Wang, and P. Ghanta, "Hermite polynomial based interconnect analysis in the presence of process variations," *IEEE Tran. on CAD*, vol. 25, no. 10, pp. 2001–2011, 2006.
- [9] D. Xiu and G. E. Karniadakis, "The Wiener-Askey polynomial chaos for stochastic differential equations," *SIAM J. Sci. Comput.*, vol. 24, pp. 619–644, 2002.
- [10] R. Winkler, "Stochastic differential algebraic equations of index-1 and applications in circuit simulation," *J. Comput. Appl. Math.*, vol. 163, pp. 435–463, 2004.
- [11] L. Arnold, "Stochastic differential equations: Theory and applications," 1974.